

The Interstellar Boundary Explorer (IBEX): Update at the End of Phase B

D.J. McComas¹, F. Allegrini¹, L. Bartolone², P. Bochsler³, M. Bzowski⁴,
M. Collier⁵, H. Fahr⁶, H. Fichtner⁷, P. Frisch⁸, H. Funsten⁹, Steve
Fuselier¹⁰, G. Gloeckler¹¹, M. Gruntman¹², V. Izmodenov¹³, P.
Knappenberger², M. Lee¹⁴, S. Livi¹⁵, D. Mitchell¹⁵, E. Möbius¹⁴, T.
Moore⁵, S. Pope¹, D. Reisenfeld¹⁶, E. Roelof¹⁵, H. Runge¹⁷, J. Scherrer¹,
N. Schwadron¹⁸, R. Tyler¹⁷, M. Wieser¹⁹, M. Witte²⁰, P. Wurzel³, G. Zank²¹

⁽¹⁾Southwest Research Institute, P.O. Drawer 28510, San Antonio, TX 78228, USA

⁽²⁾Adler Planetarium & Astronomy Museum, 1300 South Lake Shore Drive, Chicago, IL 60605, USA

⁽³⁾University of Bern, Physikalisches Institut, Sidlerstr. 5, Bern, CH-3012, Switzerland

⁽⁴⁾Polish Academy of Sciences, Space Research Centre, Bartycka 18 A, 00-716, Warsaw, Poland

⁽⁵⁾NASA Goddard Space Flight Center, Code 692, Greenbelt, MD 20771, USA

⁽⁶⁾University of Bonn, Auf dem Hugel 71, D-53121, Bonn, Germany

⁽⁷⁾Ruhr-Universität Bochum, Lehrstuhl IV: Weltraum-und-Astrophysic, D-44780, Bochum, Germany

⁽⁸⁾University of Chicago, 5640 South Ellis Avenue, Chicago, IL 60637, USA

⁽⁹⁾Los Alamos National Laboratory, P.O. Box 1663, Los Alamos, NM 87545, USA

⁽¹⁰⁾Lockheed Martin Advanced Technology Center, 3251 Hanover Street, Palo Alto, CA 94304, USA

⁽¹¹⁾University of Maryland, Department of Physics, College Park, MD 20742, USA

⁽¹²⁾University of Southern California, Los Angeles, CA 90089, USA

⁽¹³⁾Moscow State University, Vorob'evy Gory, Glavnoe Zdanie MGU, 119899 Moscow, Russia

⁽¹⁴⁾University of New Hampshire, Space Science Center, Morse Hall, Durham, NH 03824, USA

⁽¹⁵⁾Applied Physics Laboratory/JHU, 11100 Johns Hopkins Road, Laurel, MD 20723, USA

⁽¹⁶⁾University of Montana, Physics and Astronomy, 32 Campus Drive, Missoula, MT 59812, USA

⁽¹⁷⁾Orbital Sciences Corporation, 21839 Atlantic Blvd., Dulles, VA 20166, USA

⁽¹⁸⁾Boston University, 725 Commonwealth Avenue, Boston, MA 02215, USA

⁽¹⁹⁾Swedish Institute of Space Physics, IRF, Box 812, SE-981, 28 Kiruna, Sweden

⁽²⁰⁾Max Planck Institute für Aeronomie, Buchenweg 32, 37191 Katlenburg, Lindau, Germany

⁽²¹⁾University of California Riverside, Inst. Geophys. & Planetary Physics, Riverside CA 92521, USA

Abstract. The Interstellar Boundary Explorer (IBEX) mission will make the first global observations of the heliosphere's interaction with the interstellar medium. IBEX achieves these breakthrough observations by traveling outside of the Earth's magnetosphere in a highly elliptical orbit and taking global Energetic Neutral Atoms (ENA) images over energies from ~10 eV to 6 keV. IBEX's high-apogee (~50 R_E) orbit enables heliospheric ENA measurements by providing viewing from far above the Earth's relatively bright magnetospheric ENA emissions. This high energy orbit is achieved from a Pegasus XL launch vehicle by adding the propulsion from an IBEX-supplied solid rocket motor and the spacecraft's hydrazine propulsion system. IBEX carries two very large-aperture, single-pixel ENA cameras that view perpendicular to the spacecraft's Sun-pointed spin axis. Each six months, the continuous spinning of the spacecraft and periodic re-pointing to maintain the sun-pointing spin axis naturally lead to global, all-sky images. Over the course of our NASA Phase B program, the IBEX team optimized the designs of all subsystems. In this paper we summarize several significant advances in both IBEX sensors, our expected signal to noise (and background), and our groundbreaking approach to

achieve a very high-altitude orbit from a Pegasus launch vehicle for the first time. IBEX is in full scale development and on track for launch in June of 2008.

Keywords: Interstellar Boundary Explorer, termination shock, inner heliosheath, energetic neutral atoms, heliospheric ENAs, neutral atom imaging, Pegasus.

PACS: 96.50.Ek Heliopause and solar wind termination; 96.50.Xy Heliosphere/ interstellar medium interactions; 96.50.Zc Neutral particles

INTRODUCTION

The Interstellar Boundary Explorer (IBEX) mission has successfully completed its Phase B study and is under development for launch in June 2008. Over our year long Phase B program, the IBEX team made tremendous progress, optimizing all aspects of the payload, spacecraft, and mission. The IBEX science background and requirements were described by McComas et al.¹; our approach to measuring the heliospheric ENAs, the IBEX mission design, our spacecraft and payload, and the IBEX ground segment and Education and Public Outreach program were also briefly summarized². This paper updates selected advances in the IBEX payload design and describes our revolutionary approach to placing a small satellite into a high-altitude orbit from a Pegasus launch, for the first time. Additional information on IBEX is available at www.ibex.swri.edu.

IBEX will measure Energetic Neutral Atoms (ENAs), produced beyond the termination shock in the region of slowed, heated, and comparatively dense solar wind called the inner heliosheath. Figure 1 schematically displays the heliospheric interaction (background image) with the density color coded. The inset in the lower right corner of Figure 1 represents the charge exchange process. In this process, heliosheath ions become neutralized when they pass sufficiently close to cold (few eV) interstellar neutral atoms that are continuously flowing through the heliosphere. Newly created ENAs, which were previously heliosheath ions, are decoupled from the magnetic field and continue to propagate in whatever direction they happened to be traveling at the instant of charge exchange. The figure shows one such ion that became an ENA when it happened to be traveling inward toward an Earth-orbiting spacecraft (IBEX). The two opposing square fields-of-view (FOVs) represents $7^\circ \times 7^\circ$ pixels viewed by the IBEX sensors at one point in the spacecraft rotation. The inset in the upper left of this figure shows a simulated all-sky map with the location of those pixels in the sky.

Because IBEX is a simple, Sun-pointed spinner, it naturally views all directions perpendicular to the Sun-spacecraft line each and every spin. Such observations fill in the two crescents drawn in the all sky image (upper left inset). In addition, we repoint IBEX once each spacecraft orbit so that it maintains its Sun-pointed orientation, as the Earth orbits the Sun. This repointing rotates the plane of ENA observations, effectively filling in contiguous crescents in the sky. Each six months the rotation of the spin axis goes through 180° , producing a nearly full-sky map. These revolutionary, energy-resolved ENA images and per pixel energy spectra will disclose the global heliospheric interaction for the first time.

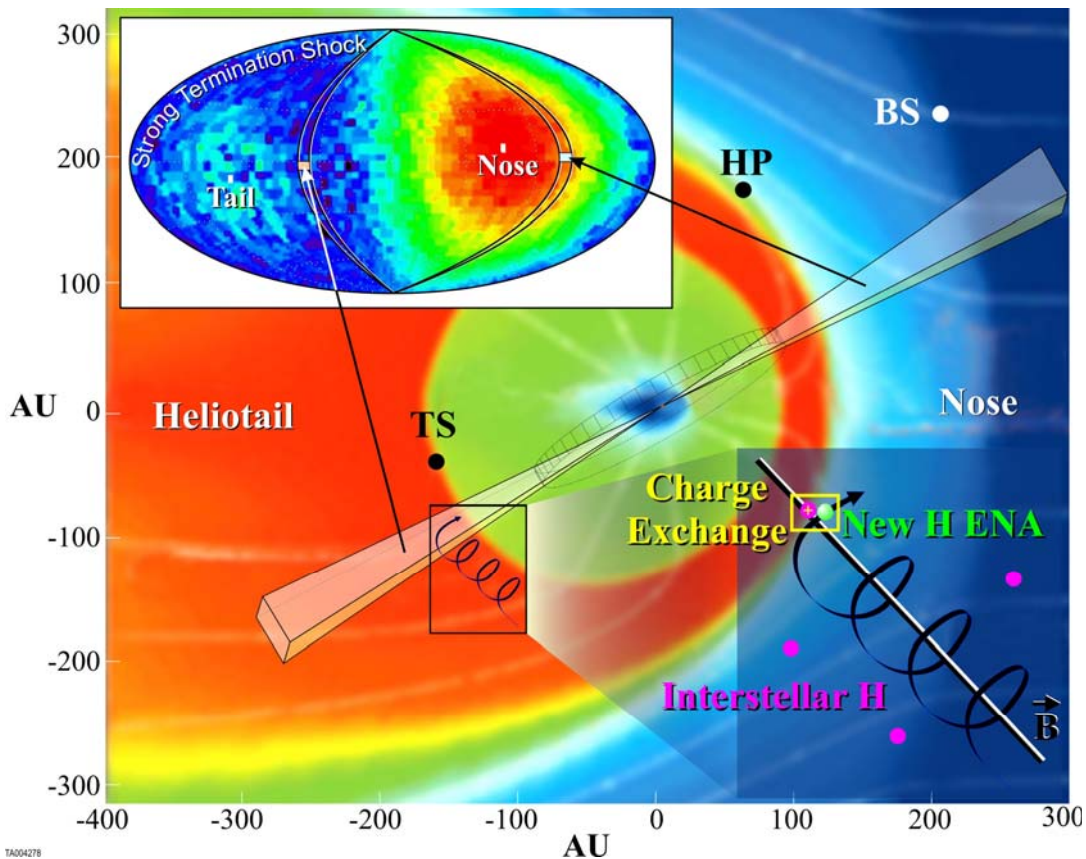


FIGURE 1. Simulated image of the heliosphere (background image) including from the inside out, solar wind (inner blue and green), termination shock (TS), inner heliosheath and heliotail (orange to yellow and outer green), heliopause (HP), interstellar medium (outer blue) and bow shock (BS). The lower right inset shows a schematic diagram of charge exchange while the upper left inset shows an all sky map and how individual pixels from the main image map onto the sky map. This image is a slightly enhanced and color version of the overall schematic shown by McComas et al.²

THE IBEX PAYLOAD

The IBEX payload is very simple and comprises only three components: two very large, high sensitivity sensors and a Combined Electronics Unit (CEU). The sensors measure ENAs from ~10 eV to 2 keV (IBEX-Lo) and from ~300 eV to 6 keV (IBEX-Hi). The CEU contains all but one of the high voltage power supplies (the last is integral to IBEX-Lo), support electronics for both sensors, and the digital data processing unit for the entire payload. The CEU also includes data storage for the entire IBEX spacecraft.

The principle of operation for the two sensors is the same² and is summarized here briefly. ENAs enter the sensors through collimators that suppress external electrons below ~600 eV and external ions below 10 keV. The collimators also set the ENA FOVs and are optimized for measurements of heliospheric ENAs from the inner heliosheath with 7° x 7° FWHM resolution. In addition, a fourth of the aperture area

for IBEX-Lo has four times the angular resolution ($3.5^\circ \times 3.5^\circ$ FWHM), which is included to precisely measure the cold interstellar neutral oxygen drifting into the heliosphere.

Just as charge exchange produces ENAs in the inner heliosheath, the two IBEX sensors use charge exchange to convert these ENAs back into ions so that they can be analyzed and detected. In the case of IBEX-Lo, this conversion produces negative ions during reflection from an ultra-smooth diamond-like carbon (DLC) surface. For IBEX-Hi charge exchange to produce positive ions occurs during transmission of the ENAs through ultra-thin (~ 10 nm) carbon foils³. Following their respective conversion subsystems, both sensors have electrostatic analyzers to select energy per charge passbands and triple coincidence detector sections; IBEX-Lo also includes time-of-flight analysis of the detected particles.

One of the major advances during our Phase B study was the optimization of the entrance subsystem for both sensors. Figure 2 shows a schematic cross section of a cut through one side of the entrance subsystem for IBEX-Lo (the IBEX-Hi collimator is nearly identical). This subsystem contains 1) the collimator (blue), which comprises a stack of thin metal plates (white lines) with precision holes that collimate the FOV, as flown on the ACE SEPICA instrument⁴, 2) electron suppressing electrodes (gold), and 3) an integrally designed sun shade (grey) and mechanical structure (green and yellow).

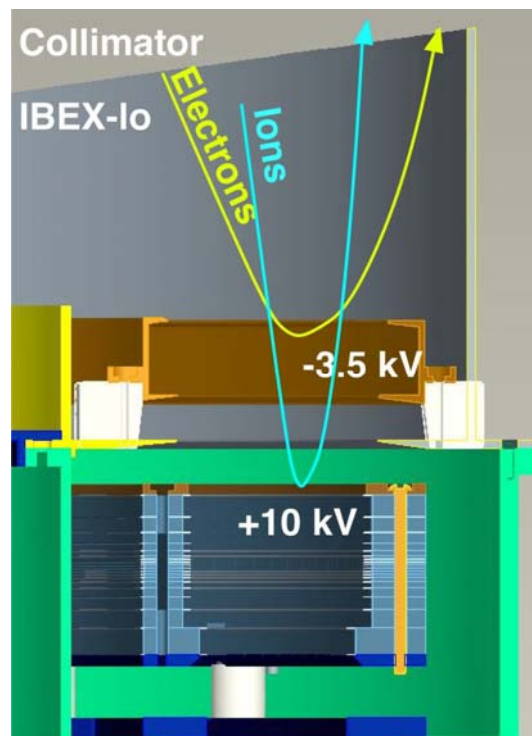


FIGURE 2. Cross section through the IBEX-Lo entrance subsystem. Electrons below ~ 600 eV and ions below 10 keV/q are reflected and cannot enter the IBEX sensors. The integral sun shade ensures no solar illumination while the collimators set the angular FOVs for the observations.

Our original design required that some of the plates be held at different voltages; +10 kV on the front plates would exclude all external ions with energies $<10 \text{ keV}/q$, while negative voltages on some of the internal plates would suppress electrons. This design had two main difficulties: first, the high external positive voltage would suck in ambient electrons, including the copious photo-electrons generated on the sunlit portions of the spacecraft surface, and second, multiple voltages on different collimator plates required a complicated insulator design for the precision stack-up of the collimator plates. Our new design suppresses the electrons first, using negative electrodes that are out of view of the incoming particle paths. This innovation allows the entire collimator stack to be floated at +10 kV as a unit. The new design is greatly simplified and provides even better rejection of charged particles, and the backgrounds they produce.

In addition to improvements in the Hi and Lo collimators, we refined the remainder of both sensor designs, simplifying what we are building and improving the mission's performance. For IBEX-Lo, tests showed that the DLC surfaces produce long-term stable conversion efficiency and that a planned heater was not required to maintain these surfaces; this progress resulted in a significantly simplified conversion subsystem design. The ion optics in IBEX-Lo were also simplified using extensive and detailed ray tracing that allowed us to combine and even eliminate several internal electrodes. Testing of the magnet configuration verified that low energy electrons produced on the conversion surfaces would be well trapped, both providing the low noise levels required for our measurements and ensuring the viability of ENA measurements all the way down to IBEX-Lo's 10 eV threshold. For the critical and somewhat complicated TOF section, we fabricated and began testing an engineering test unit during Phase B. Finally, the overall flight design of IBEX-Lo was fully matured.

In parallel, the IBEX-Hi design matured, ensuring the readiness of both sensors for full-scale flight development. A major step forward for IBEX-Hi was the demonstration that the charge conversion ultra-thin carbon foils could pass the qualification level acoustic environment. This test was so successful that it demonstrated that an acoustic cover door would not be required for this sensor. Similar to the process for IBEX-Lo, we used extensive ray trace simulations to simplify the IBEX-Hi electro-optics, even finding a way to mount the charge conversion foils at ground potential instead of having to float them at the originally planned -4.5 kV. We also further reduced the background levels by adding a high transparency grid to suppress any photoelectrons that may be produced within the collimator. Another design improvement allowed us to optimize the venting paths and separate the venting for the collimator, electro-optics, and the detector sections. Finally, we added a very small ion background monitor that will provide independent measurements of the energetic ion fluxes (roughly $>10 \text{ keV}$) around the IBEX spacecraft.

Because of the low fluxes of heliospheric ENAs, the IBEX team has put tremendous effort into quantifying and tracking all possible noise and background

sources. For these purposes we define noise as anything that generates uncorrelated (non-coincident) counts in the sensor detectors. Examples of noise sources include UV light, X-rays, penetrating radiation, and photo and secondary electrons. We use the term background for anything that can produce correlated detector counts and thus masquerade as a signal ENA in the IBEX sensors. External and internally generated ions and neutral atoms produce backgrounds. Table 1 lists the various noise and background sources that are quantified in our analysis.

Table 1. Potential noise and background sources for IBEX measurements.	
Noise Source	Background Source
Diffuse UV, UV from stars	ENAs from planetary magnetospheres
X-rays from photo-electron acceleration toward, and impact with, biased collimator grids	Ions from magnetosheath and foreshock
Photoelectrons and secondary electrons generated at conversion surface	Charge exchange of plasma ions with outgassing spacecraft species
Spacecraft Photoelectrons (e.g., from the front side of the spacecraft) that enter the collimator	ENAs from CMEs, CIRs, and pickup ion charge exch. in the heliosphere
Penetrating radiation: radionuclide decay in detectors	Secondary ions generated in entrance subsystem
Penetrating radiation: cosmic rays	
Penetrating radiation: solar energetic particle events	
Penetrating radiation: magnetospheric energetic particles	

While the details of our noise and background calculations are far too extensive to include in this brief update, the resultant expected signal-to-noise (and background) ratio from our calculations is shown in Figure 3. In this figure we use calculated heliospheric ENA emission for the bounding cases of strong and weak termination shocks⁵. Recent observations from Voyager 1 as it crossed the termination shock and in the inner heliosheath⁶⁻⁹ indicate an intermediate strength shock, which will likely have even higher emissions than shown in Figure 3. Note for comparison in this figure that the ground breaking observations of microwave background radiation made by the COBE mission¹⁰ were done with a signal to noise ratio of only 2.

IBEX LAUNCH APPROACH AND MISSION DESIGN

Another major advancement for the IBEX mission during our Phase B study was the optimization and detailed development of the methodology for getting a spacecraft into high altitude orbit from a Pegasus launch vehicle. Maximizing the apogee altitude is particularly important for IBEX because of the relatively bright ENA emissions from the Earth's magnetosphere and background contamination that may be generated in the magnetosheath and foreshock regions. At the time of our original proposal, the average expected apogee altitude for IBEX was 37 R_E, with +/- 3σ values from ~25-50 R_E. While the IBEX mission can achieve all of its groundbreaking science from an orbit with apogee as low as 25 R_E, science observations become increasingly better as the apogee is raised. Thus, it was a major goal of our Phase B effort to find a way to optimize the launch and mission design to maximize the chances of the highest possible apogee (within our 50 R_E engineering upper bound).

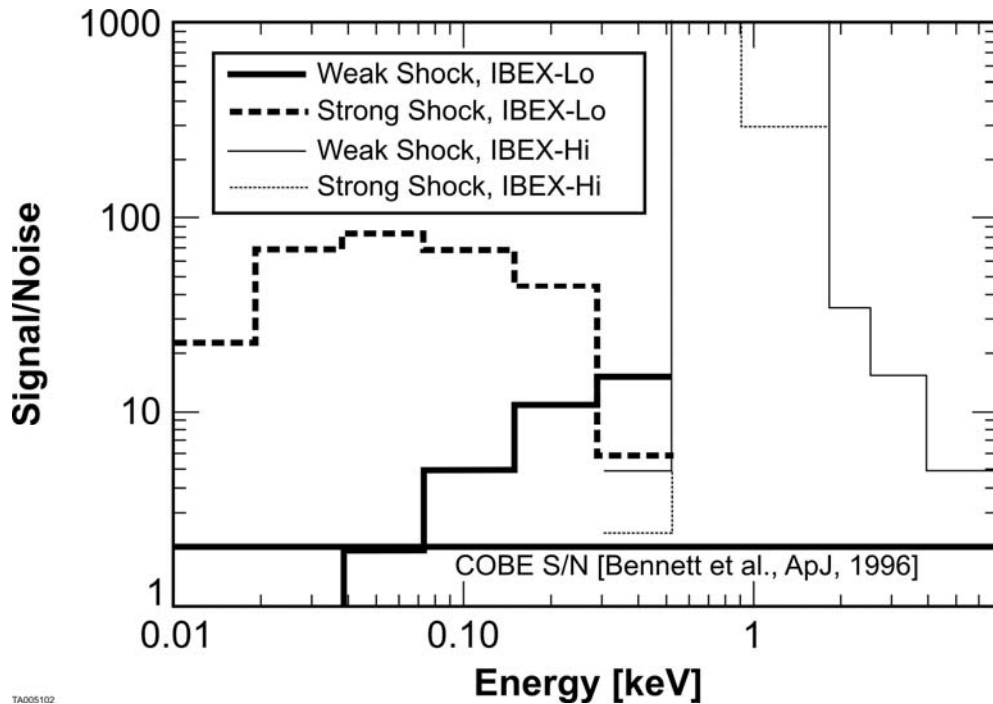


FIGURE 3. Calculated heliospheric signal to noise (plus background). The response for IBEX-Lo (thick lines) and IBEX-Hi (thin lines) is shown for the limiting cases of strong (dashed) and weak (solid) shocks⁵. For comparison, the COBE all-sky maps¹⁰ were carried out with an S/N of ~ 2 .

Our approach for getting IBEX into its high altitude orbit from a standard Pegasus XL rocket is summarized in Figure 4. The launch is planned from Kwajalein Atoll at $\sim 11^\circ$ N latitude. While more remote (and expensive), launching from this site is presently planned as launch from the Kennedy Space Center in Florida ($\sim 28^\circ$ N latitude) would provide less rotational energy of the Earth compared to a launch nearer the equator; this difference makes a small but important improvement in the total mass that the Pegasus can carry to orbit.

Pegasus will deliver IBEX to ~ 200 km altitude, point it in the desired direction, spin it up to ~ 60 RPM, and release it. After discarding a light and well balanced adapter cone, the IBEX STAR-27 solid rocket motor (SRM) will fire, carrying IBEX into a medium altitude ($\sim 15 R_E \times 200$ km) parking orbit. After similarly discarding the spent SRM casing, IBEX will use its internal hydrazine system over several orbits to raise apogee to $\sim 50 R_E$ and perigee to ~ 7000 km, above the inner radiation belt. This $\sim 50 R_E \times 7000$ km initial orbit (it evolves over time owing to the effects of solar and lunar gravitation) is ideal for IBEX's heliospheric ENA imaging. Monte Carlo calculations based on our not-to-exceed mass, full dispersions for the Pegasus and SRM thrust, and an accounting of numerous small energy losses indicates a $>99\%$ probability of achieving the $\sim 50 R_E$ apogee orbit.

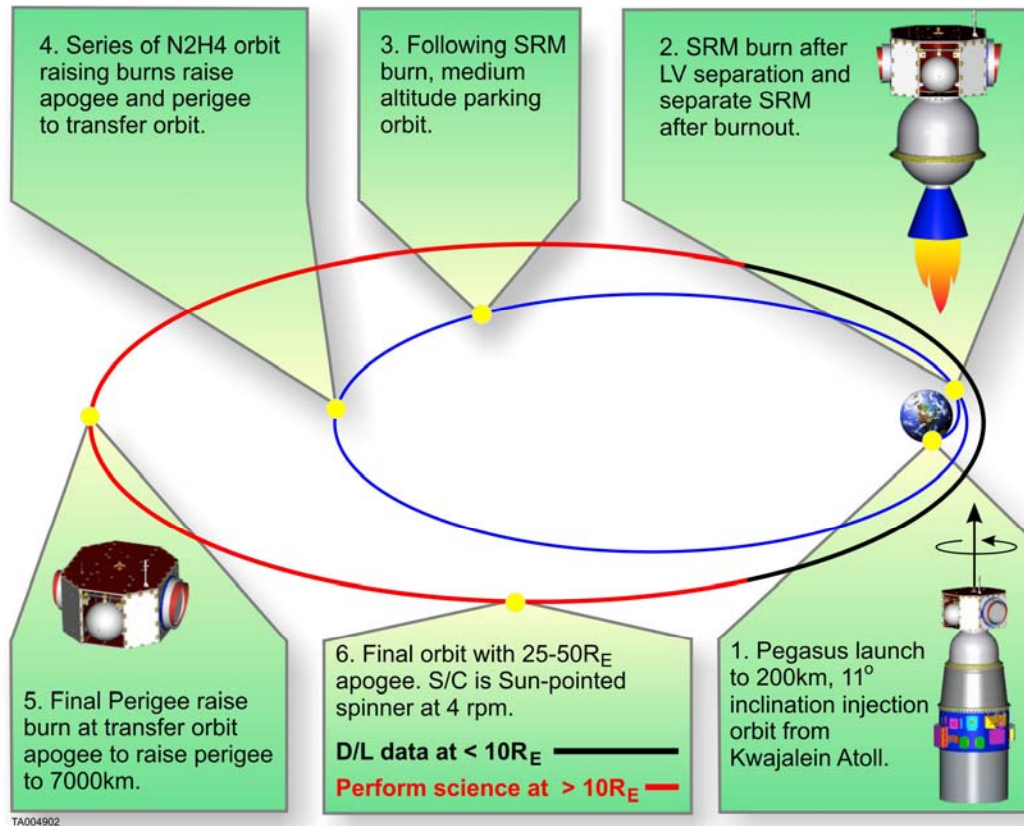


FIGURE 4. Summary of IBEX launch, orbit raising, and normal operations. Our optimized method for using a standard Pegasus XL, solid rocket motor, and on-board propulsion will allow a very high apogee orbit from a Pegasus launch vehicle for the first time. Simulations indicate a >99% probability of achieving an initial orbit of 50 R_E x 7000 km. Science measurements are taken above ~10 R_E, while the brief low altitude portion of each orbit is used for commanding, down-linking data, and reporting the spacecraft.

Because IBEX is a simple, nearly Sun-pointed spinner, the mission design allows for very simple and repetitive operations. Each ~8 day orbit IBEX makes observations at all altitudes above ~10 R_E. As IBEX re-approaches Earth, we lower the high voltages and put the sensors in a low power safe mode. Somewhere in the several-hour-long low altitude segment of each orbit (<10 R_E), 1) the IBEX spin axis (which will have drifted to ~4° east of the Sun over the previous orbit) is re-pointed back to ~4° to the west of the Sun, 2) the data from the previous orbit is downlinked, and 3) new commands for the following two orbits are uploaded. As IBEX rises back toward ~10 R_E the sensors are re-energized and begin making heliospheric ENA measurements again. Essentially all orbits follow the same simple, repetitive process and the nearly all-sky images are built up each half year of operation.

CONCLUSIONS

Over the course of Phase B, the IBEX team completed the optimization of the payload, spacecraft, ground system, and all other elements of our mission. Improvements in the entrance subsystem and both sensors have simplified the designs, reduced the already low noise and background sources, and made the designs even lower risk for full-scale development.

Our optimization of the launch and orbit raising process has produced a new and robust method for launching spacecraft into high altitude orbits from a standard Pegasus XL rocket. This approach could be used to fly a whole new range of small, relatively inexpensive missions for NASA and other sponsors by leveraging the capabilities of the Pegasus launch vehicle. Once a spacecraft has reached $\sim 50 R_E$, like IBEX, it is very nearly at full escape energy from Earth orbit. Our approach can enable not just high altitude Earth-orbiting missions, but also missions to the Moon, interplanetary space, and potentially even other planets.

The IBEX mission is on track for our planned launch in June 2008. The team is fully up to speed and making great progress developing the IBEX mission and pushing forward to accomplishing our goal of making the first global, energy resolved ENA measurements and images of the outer heliosphere and its interaction with the local interstellar medium.

ACKNOWLEDGEMENTS

Credit for the progress in the development of the IBEX Small Explorer mission is entirely due to the tremendous contributions of all IBEX Team members. In addition to our formal science team, many other scientists have joined the IBEX team and have made important additional contributions. The Engineering Team includes scientists, engineers, technicians, and business and support professionals at all of our hardware contributing institutions: Southwest Research Institute, Orbital Sciences Corporation, Lockheed Martin Advanced Technology Center, Los Alamos National Laboratory, University of New Hampshire, JHU Applied Physics Laboratory, Goddard Space Flight Center (GSFC), University of Bern, and Alliant Techsystems, Inc. While the list of individual names is far too long to include in such a short paper, our most sincere thanks go out to all of the contributors to IBEX! IBEX is supported by NASA with launch support from the Kennedy Space Center and oversight from the GSFC Explorers Program Office.

REFERENCES

1. D.J. McComas et al., The Interstellar Boundary Explorer (IBEX), *Physics of the Outer Heliosphere, Third Annual IGPP Conference*, AIP CP719, eds. V. Florinski, N.V. Pogorelov, G.P. Zank, pp. 162-181, 2004.
2. D.J. McComas et al., The Interstellar Boundary Explorer (IBEX) mission, *Proceedings Solar Wind 11 – SOHO 16 "Connecting Sun and Heliosphere"*, (ESA SP-592, September 2005), pp. 689-692, Whistler, Canada, June 2005.
3. D.J. McComas, et al., Ultra-thin (~10 nm) carbon foils in space instrumentation, *Rev. Sci. Instrumen.*, **75(11)**, pp. 4863-4870, 2004.
4. E. Moebius et al., The Solar Energetic Particle Ionic Charge Analyzer (SEPICA) and the Data Processing Unit (S3DPU) for SWIC, SWIMS, and SEPICA, *Space Sci. Rev.*, **86**, pp. 449-495, 1998.
5. Gruntman, M., et al., Energetic neutral atom imaging of the heliospheric boundary region, *J. Geophys. Res.*, **106**, pp. 15,767-15,781, 2001.
6. E.C. Stone et al., Voyager 1 explores the termination shock region and the heliosheath beyond, *Science*, **309**, p. 2017, 2005.
7. R.B. Decker et al., Voyager 1 in the foreshock, termination shock, and heliosheath, *Science*, **309**, p. 2020, 2005.
8. D.A. Gurnett and W.S. Kurth, Electron plasma oscillations upstream of the solar wind termination shock, *Science*, **309**, p. 2025, 2005.
9. L.F. Burlaga et al., Crossing the termination shock into the heliosheath: Magnetic fields, *Science*, **309**, p. 2027, 2005.
10. C.L. Bennett et al., Four-year COBE DMR cosmic microwave background observations: Maps and basic results, *Astrophys. J. Lett.*, **464**, p.L1, 1996.